Changes in Smoke-Taint Volatile-Phenol Glycosides in Wildfire Smoke-Exposed Cabernet Sauvignon Grapes throughout Winemaking

Andrew Caffrey,[1,2] Larry Lerno,[1,2] Arran Rumbaugh,[1] Raul Girardello,[1] Jerry Zweigenbaum,[3] Anita Oberholster,[1] and Susan E. Ebeler[1,2]*

Abstract: When grapes are exposed to wildfire smoke, several smoke-related aroma compounds can be transferred to the berries and become glycosylated. Although the compounds do not contribute to grape aroma in the glycosylated form, the free volatile phenols can be released throughout winemaking and wine aging to produce undesirable "smoke tainted" wines. Measurement of the intact glycosides provides insight on the potential flavor of a wine and provides information on the effect of winemaking practices on release of volatile aroma compounds from glycosidic precursors. Smoke taint-associated volatile-phenol glycosides in *Vitis vinifera* cv. Cabernet Sauvignon grape berries were tentatively identified and semi-quantitated using a comprehensive database coupled with ultra-high performance liquid chromatography and accurate-mass time-of-flight tandem mass spectrometry. Eight trisaccharide volatile-phenol glycosides were tentatively identified for the first time in grapes. The method developed here was applied to monitor changes associated with smoke exposure in 31 volatile-phenol glycosides during winemaking. The most hydrolytic time period during the winemaking process was the first half of fermentation with *Saccharomyces* yeast (EC-1118), after which there was little effect on the phenolic glycosidic profile of fermenting wines. This is the first report to monitor changes of these 31 phenolic glycosides during winemaking using direct measurement of the glycosides. The information can be used to improve knowledge of the changes in smoke-taint glycosides and release of phenolic compounds that affect sensory properties of smoke-affected grapes and wines.

Key words: Cabernet Sauvignon, fermentation, glycosides, smoke taint, ultra-high performance liquid chromatography high resolution tandem mass spectrometry, volatile phenols

As fires near grapegrowing regions increase in frequency, there is a need to understand how smoke exposure affects the fruit of *Vitis vinifera*, particularly the incidence of undesirable "smoke taint" aromas in the finished wines. The sensory characteristics of smoke taint have been well studied to date and are described as orthonasal aromas such as smoky, dirty, band-aid, earthy, medicinal, burnt/charred, muddy, tarry, smoked meat, or ashtray, along with ashtray-like retronasal aromas (Kennison et al. 2007, Ristic et al. 2011, Parker et al. 2012, Mayr et al. 2014). A class of molecules called volatile phenols have been shown to contribute to these ortho- and retro-nasal aromas in the wine. These aromas can be imparted into the grape berries in as little as half an hour of smoke exposure under intense experimental applications of smoke from burning straw (Kennison et al. 2008, Hayasaka et al. 2010a). Upon smoke exposure, free volatile phenols distribute themselves evenly throughout the pericarp of the berry (Hayasaka et al. 2010b, Dungey et al. 2011).

Guaiacol and 4-methylguaiacol are the most well-known markers of smoke taint. However, a search of the literature shows that several other volatile phenols should be considered, including, but not limited to, phenol, cresol, 4-ethylphenol, 4-ethylguaiacol, syringol, 4-methylsyringol, and eugenol (Kennison et al. 2007, 2008, Ristic et al. 2011, Hayasaka et al 2013, Noestheden et al. 2018). During smoke exposure, volatile phenols are absorbed into the grape tissue and glycosylated as a form of storage and detoxification. As a result, the volatile phenols are largely immobilized in the grape tissue (Hayasaka et al. 2010a) as monoglucosides, pentosylglucosides, gentiobiosides, and rutinosides (Hayasaka et al. 2013). In finished wines, the abundance of each volatile phenol is proportional to the duration and amount of smoke exposure on the grapes, as well as the timing of smoke exposure during grape growth. Previous studies have shown that even a single exposure to smoke starting three to 24 days postveraison can impart a significant amount of volatile phenols into the berries (Kennison et al. 2009).

Most studies utilize the same glycosylation motifs for volatile phenols that have been observed for other volatiles, such as monoterpene alcohols and norisoprenoids. Much of the

[1]Department of Viticulture and Enology, University of California, Davis, CA; [2]Food Safety and Measurement Facility, University of California, Davis, CA; and [3]Agilent Technologies, Inc., Wilmington, DE 19898.

*Corresponding author (seebeler@ucdavis.edu)

Acknowledgments: We acknowledge the American Vineyard Foundation for financial support of this work.

Supplemental data is freely available with the online version of this article at www.ajevonline.org.

Manuscript submitted Dec 2018, April 2019, accepted May 2019

doi: 10.5344/ajev.2019.19001

focus has been on the glucose-containing monosaccharides and disaccharides listed above in model systems, grapes, or finished wines (Kennison et al. 2008, 2009, Hayasaka et al. 2010a, 2010b, 2013, Dungey et al. 2011, Wilkinson et al. 2011). However, that approach may not address any deviations from the typical glucose-containing mono- and disaccharide motif, such as non-glucoside and trisaccharide glycosides, as seen by Noestheden et al. (2018), who recently characterized non-glucose containing glycosides in grapes and wines. A broader search for bound smoke-taint phenols has not been reported. This study aims to continue the characterization of glycosylated volatile phenols (referred to hereafter as volatile-phenol glycosides) through the use of tandem mass spectrometry (MS/MS), and to expand the knowledge of how these individual glycosides change during the winemaking process.

Materials and Methods

Chemicals/reagents and sample preparation materials. All water used during the experiments was 18 MΩ·cm deionized water from a Milli-Q Element system (Millipore). Liquid chromatography/mass spectrometry (LC/MS)-grade acetonitrile, ACS reagent grade sodium hydroxide, and high-performance liquid chromatography-grade glacial acetic acid were purchased from Fisher Scientific. Salicin (99+%) was purchased from Sigma Aldrich. Strata-X solid-phase extraction (SPE) cartridges were purchased from Phenomenex. Plexa SPE cartridges were provided by Agilent Technologies.

Grapes, winemaking, and sampling. Cabernet Sauvignon grapes were harvested from UC Davis Oakville Vineyards (Napa County, CA) from 110R and 420A rootstocks on 17 Oct 2017, with ~10 days of exposure to smoke from the 2017 Napa County fire. The grapes were harvested at a soluble solids of 25.0 Brix, pH 3.67, 4.6 g/L titratable acidity (tartaric acid equivalents), and a yeast assimilable nitrogen content of 147 g N/L. The grapes were harvested and immediately destemmed, crushed, and divided into three replicate fermentation vessels at the UC Davis Teaching and Research Winery (Davis, CA). Once divided, a 15% potassium metabisulfite solution was used to add 50 mg/L total sulfur dioxide (SO_2) to the must. The must samples were then manually mixed.

The must samples were held at 25°C in jacketed stainless steel fermentor tanks controlled by an integrated fermentation control system for 24 hr before inoculation with EC-1118 yeast (Lallemand Lalvin). Once the fermentations commenced, two fermentor volumes of juice were pumped over two times/day. From inoculation, the fermentations were held at 25°C for a total of eight days with skin and seed contact until the measured residual sugars were below 3 g/L according to enzyme analysis. The wines were pressed with a Cypress Semiconductor Corporation hydraulic basket press to remove the skins and seeds. Malolactic fermentation was initiated with the addition of Viniflora *Oenococcus oeni* (Chr. Hansen A/S). The wines were stored at 12°C with an adjusted free SO_2 of 30 mg/L after malolactic fermentation was completed. The duration of malolactic fermentation was ~5 mo. The wines were then sterile filtered and bottled into Bordeaux bottles with screwcaps lined with Saranex inner films (Saraflex). The wines were filtered with a nominal and an absolute filter. The nominal filter was a Filtrox Fibrafix AF 71H 1.5- to 3-µm cellulose acetate filter pad and two Filtrox AF 101H 0.6- to 0.8-µm cellulose acetate filter pads. The absolute filter was a Vitipore II canister and cartridge system with a 0.45-µm polyvinylidene fluoride Durapore membrane.

During the winemaking, several samples were taken. Two representative grape clusters were sampled every 5 min off a shaker table during grape processing. Grapes were pulled at several different places across each cluster to total 2.5 kg of grapes. Duplicate 50-mL samples were taken from each replicate fermentation at the following four time points during the primary fermentation: after the grapes were processed and crushed, at the start of the primary fermentation after ~24 hr (~25.0 Brix), during the middle of the primary fermentation (12.5 ± 1.0 Brix), and at the conclusion of the primary fermentation (<0 Brix). The last set of samples were taken at the conclusion of winemaking as the wines were bottled. Between the primary fermentation and bottling stage, the wines had undergone malolactic fermentation, racking, and filtration. Fermentation samples were taken during a pump-over cycle to ensure a homogenous juice sample. All samples were immediately frozen at -80°C, and one of the two duplicate samples was analyzed within one year of freezing, while the other remained frozen as a precautionary measure for back-up analysis, if needed.

Sample preparation. Prior to SPE, grape berries were prepared according to the method of Hjelmeland et al. (2015). Three separate ~25-g samples of frozen berries were cryo-ground to a powder using an IKA A11 basic analytical mill (IKA Works, Inc.). Approximately 5 g of berry powder from each replicate was accurately weighed into a 50-mL centrifuge Falcon tube (Fisher Scientific). A 5-mL aliquot of a pH 5, 50 mM sodium citrate buffer was added to the same centrifuge tube, and the grape powder was allowed to thaw to room temperature. The samples were then centrifuged at 4°C at 4100 × *g* for 15 min in an Eppendorf 5403 centrifuge. Samples were strained through a cheesecloth into a new clean centrifuge tube and centrifuged again under the same conditions. Each replicate fermentation sample obtained during the winemaking process was removed from the freezer, brought to room temperature, and centrifuged one time under the same conditions.

After centrifugation, a 5-mL aliquot of the grape extract or fermentation sample supernatant was placed into a new centrifuge tube and spiked with a salicin internal standard to obtain a salicin concentration of 50 µg/L. The solution was vortexed to mix and used for SPE. SPE was performed in triplicate following the method proposed by Noestheden et al. (2018) with minor changes. Two SPE phases were tested for reproducibility and extractability. The first phase was a Phenomenex Strata-X 200 mg, 3 mL SPE cartridge, and the second phase was an Agilent Bond Elut Plexa 200 mg, 3 mL SPE cartridge. The following was used for the extraction steps: 2 mL of acetonitrile for conditioning, followed by 2 mL of water, 1 mL of grape sample, 1 mL of 0.1 M NaOH solution, and an additional 2 mL of water. The phenolic

glycosides were eluted from the column with 2 mL of 40% acetonitrile in water. The eluent was dried at 35°C under vacuum and reconstituted in 1.0 mL of water for analysis. Samples were stored at -20°C and analyzed within 2 wks of storage.

UHPLC-qTOF MS analysis. The resulting extracts were analyzed using an Agilent 1290 Infinity ultra-high-performance liquid chromatography (UHPLC) system coupled with an Agilent 6545 quadrupole time-of-flight (Q-TOF) LC/MS. Samples were held in the auto-sampler at 8°C for analysis. A 10-µL injection of the extract was analyzed on an Agilent Poroshell 120 Phenyl-Hexyl 2.1 mm × 150 mm, 2.7-µm particle size column with an Agilent Poroshell 120 Phenyl-Hexyl 2.1 mm × 5 mm, 2.7-µm particle size guard column. The column compartment was heated to 40°C for the analysis. Mobile phase A consisted of 0.1% acetic acid in water, and mobile phase B consisted of 0.1% acetic acid in acetonitrile with a flow rate of 0.42 mL/min. The solvent gradients followed a linear gradient from 5% B to 35% B over the course of 10 min, increased to 95% B over 10 min, and returned to 5% B over 2 min, followed by re-equilibration of the column for 5 min at 5% B.

For the MS analysis, electrospray ionization (ESI) and atmospheric pressure chemical ionization (APCI) sources were compared. For ESI, samples were analyzed in negative mode on an Agilent Dual ESI Jet stream source. The sheath gas was N heated to 350°C at 12 L/min. The drying gas was N at a temperature of 100°C with a flow rate of 10 L/min. The capillary voltage was set to 3500 V with a fragmentor voltage of 120 V, nozzle voltage of 500 V, and a nebulizer set to a pressure of 35 psig. The instrument was tuned to the manufacturer's specifications in high-resolution mode.

An Agilent APCI source was used for the APCI analysis. The gas temperature was set to 350°C with a flow rate of 8 mL/min. The vaporizer temperature was set to 350°C, and the nebulizer pressure was 35 psig. The capillary voltage was 4000V, the fragmentor voltage was set to 75V, and the corona current was 5 µA in negative mode.

Reference ions were used for a continuous mass calibration during each run. A reference mass solution containing proton abstracted purine (*m/z* 119.0362) and the acetate adduct of hexakis (1H,1H,3H-tetra-fluoropropoxy)phosphazene (*m/z* 980.016375) was sprayed into the source at a rate of 4 µL/min through the second sprayer in the dual ESI source. This solution was introduced with a tee in the LC eluent directly before the APCI sprayer.

MS/MS spectra were obtained through the Auto MS/MS function on the instrument. Source conditions were the same as single MS acquisitions. Different collision energies were used for fragmentation depending on the number of sugars in the glycoside. Monosaccharides required a collision energy of 10 eV, whereas disaccharides and trisaccharides required collision energies of 20 eV and 30 eV, respectively. The scan range for MS was *m/z* 100 to 1000 with a scan rate of 3 spectra/sec. For MS/MS, the range was *m/z* 50 to 750 with a scan rate of 4 spectra/sec. Precursors were selected with a narrow isolation width of 1.3 amu with a maximum of three precursors/cycle. Active exclusion was enabled after five scans and released after 0.5 min.

Data analysis and workflow. A comprehensive list of volatile phenols identified in smoke-exposed grapes was created based on previously published information (Kennison et al. 2007, 2008, Dungey et al. 2011, Ristic et al. 2011, Hayasaka et al. 2013, Noestheden et al. 2018). The sugars apiofuranose, arabinofuranose, rhamnopyranose, xylopyranose, galactopyranose, and glucopyranose were considered as potential sugars for glycosylation (Sarry and Günata 2004, Dziadas and Jelén 2011, Bönisch et al. 2014). Apiofuranose, arabinofuranose, and xylopyranose were generalized as pentose sugars. Glucopyranosyl and galactopyranosyl were generalized as hexose sugars, and rhamnopyranosyl was generalized as a deoxyhexose sugar. Glycosides of up to three sugars were considered. All possible glycosides were drawn using Marvinsketch and imported into the Agilent MassHunter Personal Compound Database Library (PCDL) Manager. Using the personal compound database (PCD) of formulas, the exact molecular masses were generated automatically within the software. Each compound was given a name based on the sugars of the glycoside and the volatile phenol it contained, e.g., deoxyhexose-hexose-4-methylguaiacol.

Grape samples were used to generate MS^1 data and analyzed with Agilent MassHunter Qualitative Analysis. The Qualitative Analysis Find-By-Formula algorithm was used to search against the PCD to find masses of deprotonated or acetate adduct ions. Ions that were found with a mass error less than 10 ppm from the theoretical mass and an appropriate isotope spacing associated with the proposed formula, adduct, and/or fragment were identified. A list containing all potential compounds was exported from the software as an inclusion list for MS/MS. MS/MS spectra were generated to tentatively identify compounds. Agilent MassHunter Molecular Structure Correlator (MSC) was then used as an aid to interpret and tentatively identify compounds based on the 30 most abundant ions in the MS/MS spectra. Candidate molecules were displayed in the software, along with scores based on the number of fragments that could be matched to the compound, the mass error of each fragment, and likelihood of the fragment being produced from collision induced dissociation (CID). Tentative identifications through MSC were verified within the software by manual interpretation of the MS/MS spectra based on comparing the data to known fragmentation patterns of glycosylated molecules (Flamini et al. 2014, Hjelmeland et al. 2015, Ponzini et al. 2015, Noestheden et al. 2018).

Retention times and MS/MS spectra were used to make a PCDL that was used for relative quantitation. The PCDL was imported into Agilent MassHunter Quantitative Analysis where integrations were performed. Peak areas were normalized by dividing the peak area of each unique compound by the peak area of the internal standard salicin. A signal-to-noise ratio of 10 was considered for quantitation. After compounds were tentatively identified, a library was created to relate retention times and MS/MS fragmentation spectra for each of the analytes. MassHunter Quantitative

Analysis integration software utilized this library to analyze the abundance of each compound and normalized them to the internal standard salicin. After the establishment of this library, an "all ions" workflow was used for quantitation in wine samples. An "all ions" workflow involves the use of a low (0 eV) and mid-level (20 eV) collision energy during single MS analysis to allow for compound verification during the integration process in the case of matrix effects on retention times. Compounds are verified using retention time coelution with the precursor ion in the 0 eV signal and fragments in the 20 eV signal to the MS/MS fragments found in the PCDL that was created.

Statistical analysis. Sample means and standard deviations were calculated in Microsoft Excel (Microsoft). Analysis of variance (ANOVA) was calculated in R (v3.4.4, RStudio). Sample means were compared using Tukey's honestly significant difference tests. All analyses used an α of 0.05 for determining statistical significance. Results for the ANOVA analysis are reported in Supplemental Table 1.

Results and Discussion

Sample preparation. Sample preparation was based on the work of Noestheden et al. (2018), which noted that the Strata-X phase had higher recoveries of volatile-phenol glycosides than other SPE phases (Noestheden et al. 2018). This type of phase was adopted here with comparison of two different, but similar, SPE phases: the Phenomenex Strata-X (first phase) and the Agilent Bond Elut Plexa (second phase). The Strata-X phase was ultimately chosen due to a higher recovery of compounds and a smaller average relative standard deviation (RSD) (~4%) than in the Plexa phase (~9%; data not shown). Variations during the SPE and drying processes were accounted for by the internal standard salicin. Salicin was chosen because it has a similar structure as volatile-phenol glycosides, is readily available and inexpensive, and had a low RSD (~1%) during analysis. Figure 1 compares the structures of salicin and hexose-guaiacol and their separation during chromatography.

UHPLC-QTOF analysis. Positive and negative instrument polarities were evaluated. Negative mode produced more peaks for analysis and was in accordance with other studies on this topic (Hayasaka et al. 2010a, 2010b, 2013, Dungey et al. 2011, Noestheden et al. 2018). A phenyl-hexyl column (Poroshell 120 PhenylHexyl 2.1mm × 150 mm, 2.7 mm; Agilent) was chosen to allow for separation and retention via aromatic ring interactions. The mobile phases of water and acetonitrile acidified with acetic acid were used based on previous work with monoterpene glycosides and literature on volatile-phenol glycosides (Hayasaka et al. 2010a, 2010b, Dungey et al. 2011, Hjelmeland et al. 2015). The majority of compounds of similar masses were baseline resolved based on the chromatographic conditions, as demonstrated in Supplemental Figure 1.

Dual jet spray ESI and APCI were compared for analysis. Contrary to the results of Hayasaka et al. (2013), dual jet spray ESI produced a higher signal for most analytes (data not shown). Along with these results, APCI was unable to ionize trisaccharides, probably due to low volatility for ionization. Therefore, dual jet spray ESI was chosen for further analysis.

Analysis of glycosides. Applying the extraction methods and instrument parameters described above, grape samples were chosen as a representative sample for characterizing the glycosides. Up to three potential sugars were considered for each volatile-phenol glycoside: a hexose, pentose, or deoxyhexose sugar. All structures were used to make a database of masses that could be used to search for potential compounds in the grape samples. Nearly 100 possible compounds were identified in the untargeted search. Through MS/MS and the MSC software, 31 different volatile-phenol glycosides (eight monosaccharides, 15 disaccharides, and eight trisaccharides) were tentatively identified (Table 1). Tentatively identified compounds had to satisfy the typical CID fragmentation patterns for sugar-containing molecules reported previously (Flamini et al. 2014, Hjelmeland et al. 2015, Ponzini et al. 2015), i.e., characteristic ring fragmentations of sugars and the loss of terminal sugars. The glycosylation pattern

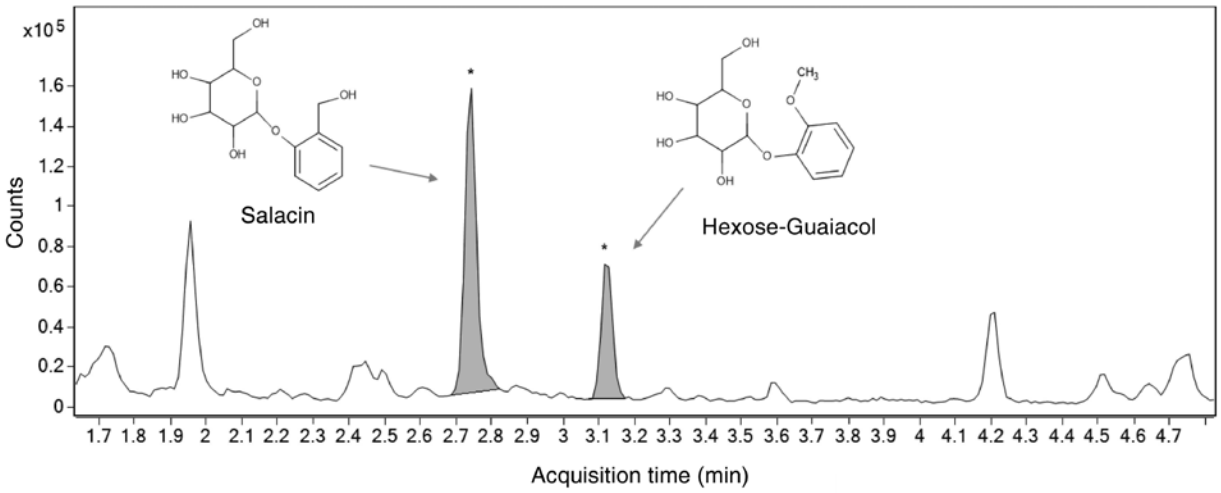

Figure 1 Extracted ion chromatogram showing peaks with *m/z* 285.0980. Salicin (left) and Hexose-Guaiacol (right) have similar structural similarities but are still fully resolved peaks.

Table 1 Tentatively identified volatile-phenol glycosides in Cabernet Sauvignon grape extracts. The chemical formula, retention time, calculated exact mass, and tandem mass spectrometry (MS/MS) ions are shown. I.S., internal standard.

	Name	Retention time (min)	Formula	Mass	m/z	MS/MS Product Ions
1	Hexose-Syringol	2.450	$C_{14}H_{20}O_8$	316.1158	315.1085	59.0139, 71.0139, 89.0244, 153.0557, 161.045, 179.0561,153.0557, 315.1085
2	Hexose-Hexose-Hexose-4-Ethylguaiacol	3.012	$C_{27}H_{42}O_{17}$	638.2422	637.2349	59.0139, 71.0139, 89.0244, 101.0244, 113.0244, 119.0350, 161.045, 179.0561, 295.1187, 457.1715, 475.1821
3	Hexose-Hexose-Pentose-4-Methylguaiacol	3.138	$C_{25}H_{38}O_{16}$	594.2160	593.2087	59.0139, 71.0139, 89.0244, 101.0244, 113.0244, 119.0350, 125.0244, 131.0350, 143.0350, 149.0455, 161.045, 179.0561, 269.1031, 323.0978, 431.1559, 593.2087
4	Hexose-Pentose-Guaiacol	3.169	$C_{18}H_{26}O_{11}$	418.1475	417.1402	59.0139, 71.0139, 89.0244, 101.0244, 113.0244, 119.0350, 125.0244, 131.0350, 143.0350, 149.0455, 161.0450, 181.0506, 255.0874, 417.1402
5	Hexose-Guaiacol	3.273	$C_{13}H_{18}O_7$	286.1053	285.0980	59.0139, 71.0139, 89.0244, 101.0244, 113.0244, 119.0350, 125.0244, 143.0350, 161.045, 179.0561, 285.0980
6	Hexose-Pentose-Pentose-4-Methylguaiacol	3.448	$C_{24}H_{36}O_{15}$	564.2054	563.1981	59.0139, 71.0139, 89.0244, 101.0244, 113.0244, 119.0350, 125.0244, 131.0350 143.0350, 179.0561, 269.1031, 401.1453, 563.1981
7	Hexose-Pentose-4-Methylguaiacol	3.577	$C_{19}H_{28}O_{11}$	432.1632	431.1559	59.0139, 71.0139, 89.0244, 101.0244, 113.0244, 119.0350, 125.0244, 131.0350, 143.0350, 149.0455, 161.045, 179.0561, 269.1031, 431.1559
8	Pentose-Pentose-Hexose-Cresol	3.700	$C_{23}H_{34}O_{14}$	534.1949	533.1876	59.0139, 71.0139, 89.0244, 101.0244, 113.0244, 119.0350, 125.0244, 131.0350, 143.0350, 149.0455, 161.045, 179.0561, 196.0589 269.1031, 533.1876
9	Pentose-Pentose-Phenol	3.784	$C_{16}H_{22}O_9$	358.1264	357.1191	59.0139, 71.0139, 89.0244, 101.0244, 113.0244, 119.0350, 125.0244, 131.0350, 225.0768, 357.1191
10	Deoxyhexose-Pentose-Phenol	3.979	$C_{17}H_{24}O_9$	372.1420	371.1348	59.0139, 71.0139, 89.0244, 101.0244, 113.0244, 119.0350, 143.0350, 149.0455 161.045, 209.0819, 371.1191
11	Hexose-Hexose-4-Methylguaiacol	4.053	$C_{20}H_{30}O_{12}$	462.1732	461.1664	59.0139, 71.0139, 89.0244, 101.0244, 113.0244, 125.0244, 131.0350, 143.0350, 161.045, 269.1031, 461.1664
12	Hexose-Hexose-Pentose-4-Ethylguaiacol	4.048	$C_{24}H_{36}O_{14}$	608.2316	607.2244	59.0139, 71.0139, 89.0244, 101.0244, 113.0244, 119.0350, 125.0244, 131.0350, 143.0350, 149.0455, 161.045, 179.0561, 323.0978, 445.1657, 607.2244
13	Hexose-Cresol 1	4.080	$C_{13}H_{18}O_6$	270.1103	269.1031	59.0139, 71.0139, 89.0244, 101.0244, 113.0244, 143.0350, 161.045, 269.1031
14	Hexose-4-Methylguaiacol	4.091	$C_{14}H_{20}O_7$	300.1209	299.1136	59.0139, 71.0139, 89.0244, 101.0244, 113.0244, 119.0350, 131.0350, 143.0350, 161.045, 179.0561, 299.1136
15	Hexose-4-Methylsyringol	4.121	$C_{15}H_{22}O_8$	330.1315	329.1242	59.0139, 71.0139, 89.0244, 101.0244, 113.0244, 143.0350, 161.045, 329.1242
16	Hexose-Hexose-Pentose-Cresol	4.185	$C_{26}H_{40}O_{17}$	624.2266	623.2193	59.0139, 71.0139, 89.0244, 101.0244, 113.0244, 119.0350, 125.0244, 131.0350, 143.0350, 145.0506, 149.0455, 161.045, 179. 179.0561. 269.1031, 401.1453, 623.2193
17	Pentose-Hexose-Cresol	4.289	$C_{18}H_{26}O_{10}$	402.1526	401.1453	59.0139, 71.0139, 89.0244, 101.0244, 113.0244, 125.0244, 131.0350, 143.0350, 149.0455 161.045, 269.1031, 401.1453
18	Hexose-Pentose-4-Methylguaiacol	4.293	$C_{19}H_{28}O_{11}$	432.1632	431.1559	59.0139, 71.0139, 89.0244, 101.0244, 113.0244, 119.0350, 143.0350, 149.0455, 161.045, 269.1031, 431.1559
19	Hexose-Pentose-4-Methylguaiacol	4.372	$C_{19}H_{28}O_{11}$	432.1632	431.1559	59.0139, 71.0139, 89.0244, 101.0244, 113.0244, 119.0350, 125.0244, 131.0350, 149.0455, 161.045, 191.0561, 269.1031, 431.1559
20	Hexose-Cresol 2	4.375	$C_{13}H_{20}O_8$	270.1103	269.1031	59.0139, 71.0139, 89.0244, 101.0244, 113.0244, 125.0244, 143.0350, 161.045, 269.1031
21	Deoxyhexose-Hexose-Cresol	4.649	$C_{19}H_{28}O_{10}$	416.1682	415.1610	59.0139, 71.0139, 89.0244, 101.0244, 113.0244, 119.0350, 125.0244, 143.0350, 145.0506, 161.045, 269.1031, 415.1610
22	Pentose-Hexose-4-Ethylphenol	5.192	$C_{21}H_{32}O_{12}$	416.1682	415.1610	59.0139, 71.0139, 89.0244, 101.0244, 113.0244, 119.0350, 125.0244, 131.0350, 143.0350, 149.0455, 179.0561, 191.0561, 283.1187, 415.1610
23	Pentose-Pentose-4-Ethylguaiacol	5.343	$C_{19}H_{28}O_{10}$	416.1683	415.1610	59.0139, 71.0139, 89.0244, 101.0244, 113.0244, 119.0350, 131.0350, 149.0455, 283.1187, 415.1610
24	Deoxyhexose-Pentose-4-Ethylguaiacol	5.810	$C_{20}H_{30}O_{10}$	430.1839	429.1766	59.0139, 71.0139, 89.0244, 101.0244, 113.0244, 119.0350, 125.0244, 131.0350, 143.0350, 145.0506, 149.0455 161.045, 429.1766
25	Deoxyhexose-Hexose-Pentose-Phenol	6.061	$C_{23}H_{34}O_{14}$	534.1949	533.1876	59.0139, 71.0139, 89.0244, 101.0244, 113.0244, 119.0350, 125.0244, 131.035, 143.0350, 145.0506, 209.0819, 371.1348, 533.1876
26	Deoxyhexose-Eugenol	6.837	$C_{16}H_{22}O_6$	310.1416	309.1344	59.0139, 71.0139, 89.0244, 113.0244,145.0506, 309.1344
27	Pentose-Pentose-Pentose-Cresol	6.983	$C_{22}H_{32}O_{13}$	504.1843	503.1770	59.0139, 71.0139, 89.0244, 101.0244, 113.0244, 125.0244, 149.0455, 209.0819, 503.1770
28	Deoxyhexose-Pentose-Pentose-Phenol	7.141	$C_{22}H_{32}O_{13}$	504.1843	503.1770	59.0139, 71.0139, 89.0244, 101.0244, 125.0244, 149.0455, 165.0921, 209.0819, 503.1770
29	Pentose-Pentose-Cresol 1	7.759	$C_{17}H_{24}O_9$	372.1420	371.1348	59.0139, 71.0139, 89.0244, 101.0244, 113.0244, 119.0350,143.0350,149.0455, 161.045, 209.082, 371.1348
30	Pentose-Pentose-Cresol 2	8.145	$C_{17}H_{24}O_9$	372.1420	371.1348	59.0139, 71.0139, 89.0244, 101.0244, 113.0244, 125.0244, 149.0455, 209.082, 371.1348
31	Deoxyhexose-4-Ethylphenol	8.455	$C_{14}H_{20}O_5$	268.1311	267.1238	59.0139, 71.0139,161.045, 179.0692, 267.1238
I.S.	Salicin	2.823	$C_{13}H_{18}O_7$	286.1053	285.0980	

of volatile phenols follows the same trends as other glycosidic aroma molecules such as monoterpene alcohols. For example, similar to other aroma glycosides, the majority of volatile-phenol glycosides fall into the disaccharide category (Flamini et al. 2014, Hjelmeland et al. 2015). There are few cases that trisaccharide glycosides have been reported for monoterpene glycosides in grapes (Hjelmeland et al. 2015). Volatile-phenol trisaccharides have been shown to be present in tomato fruit (Tikunov et al. 2010), however, this is the first tentative identification of volatile-phenol trisaccharides in grapes.

Figure 2 and Table 1 give an example MS/MS spectrum of a trisaccharide and the fragmentation masses of all of the observed glycosides in this study. Figure 2 shows the CID fragmentation pattern of a hexose-hexose-pentose-4-methylguaiacol glycoside at 30 eV. The primary fragmentations are consistent with other fragmentation studies on volatile-phenol glycosides (Noestheden et al. 2018). The figure also shows the loss of each sugar in the glycone portion of the molecule, along with the ring fragmentations typical of sugar moieties in glycosides (Hjelmeland et al. 2015). The Y_0 fragment associated with the phenol portion of the molecule was not included as a diagnostic ion due to its overall low abundance.

This is the most comprehensive report of volatile-phenol glycosides in grapes naturally exposed to California wildfires. While the overall composition is similar to previous reports in the literature, it is notable that syringol- and guaiacol-diglycosides do not predominate, as previously reported (Hayasaka et al. 2013).

Analysis of samples during fermentation. The direct analysis of volatile-phenol glycosides during the winemaking process has not been reported. Studies that have looked at the effects of fermentation on these glycosides do so through GC/MS. These studies analyzed volatile phenols before and after the primary fermentation has taken place, with and without indirect analysis of glycosides, and through induced enzyme or acid hydrolysis (Kennison et al. 2008, Ristic et al. 2011). This approach does not allow the monitoring of changes in individual glycosides as a function of endogenous grape glycosidases after the grapes are crushed, exogenous microbial glycosidases during primary and secondary fermentation, or the role of acid hydrolysis to spontaneously free the volatile phenols. Therefore, the goal of this fermentation study was to compare the abundance of volatile-phenol glycosides in grape juice at the time of crushing, throughout fermentation, and up to the time immediately before the finished wine was bottled. Figure 3A to 3C shows the effect of the winemaking process on the relative abundances of volatile-phenol glycosides. After the grapes were crushed, SO_2 was added to inhibit fermentation by native microflora. There were no statistically significant differences in glycosides between the juice at crush and the start of fermentation after one day of maceration. This lack of change from this time period shows that there was no measurable action of grape glycosidases after the grapes were crushed. Since volatile-phenols are evenly distributed between the juice and the skins (Hayasaka et al. 2010b, Dungey et al. 2011), we expected that the abundances would increase due to extraction of these compounds from

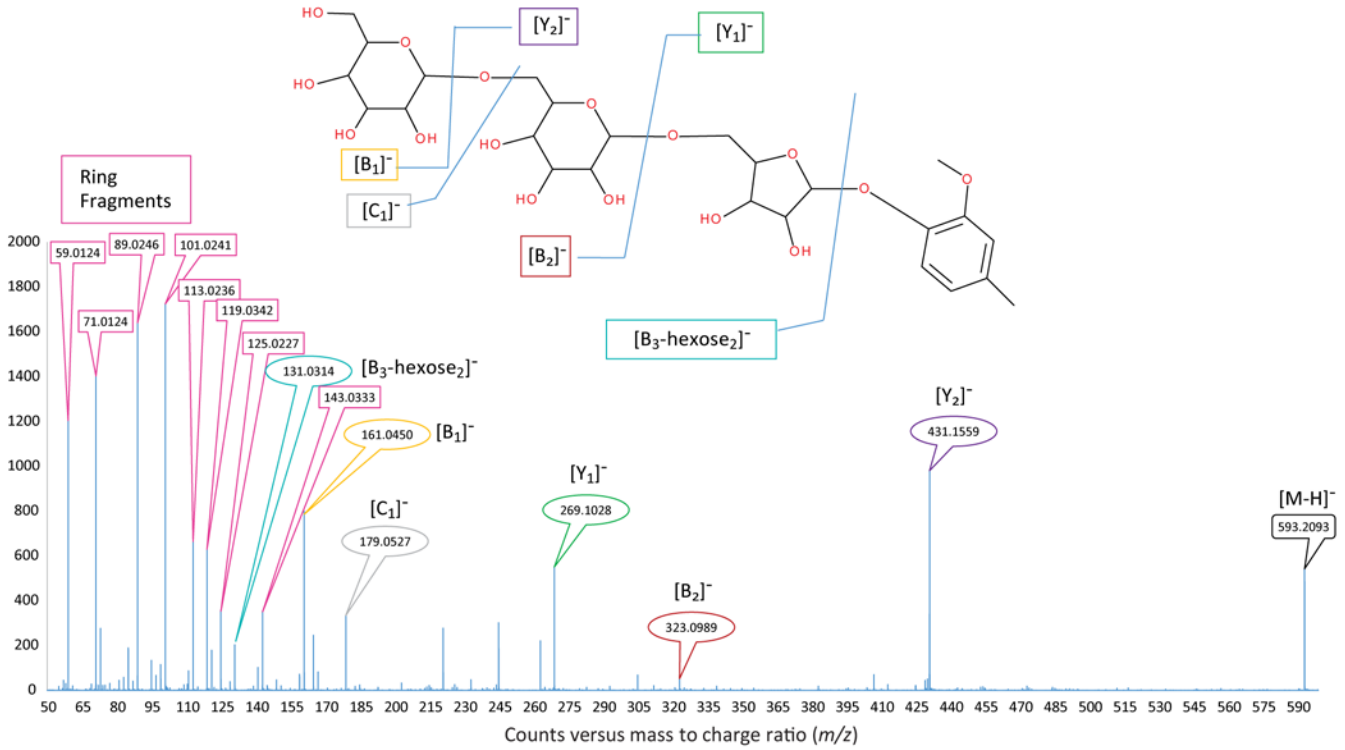

Figure 2 The fragmentation pattern of putatively identified hexose-hexose-pentose-4-methylguaiacol at 30 eV shows the characteristic ring fragments of glycosidic molecules along with several other neutral losses within the sugar and alglycone portions.

the skins, but this was not the case for any compounds in Figure 3. The relative abundance of two of the trisaccharides increased noticeably during the fermentation process (Figure 3C). The trisaccharides were not detected at the start of the fermentation; however, these compounds were found in the grape extract (Table 1). It is possible that as the fermentation continued, the glycosides were extracted from grape solids into the juice. In addition, there is a possibility of ion suppression taking place that may have affected the analysis; however, in the absence of chemical standards for each compound, future work is needed to understand how these factors affect analysis.

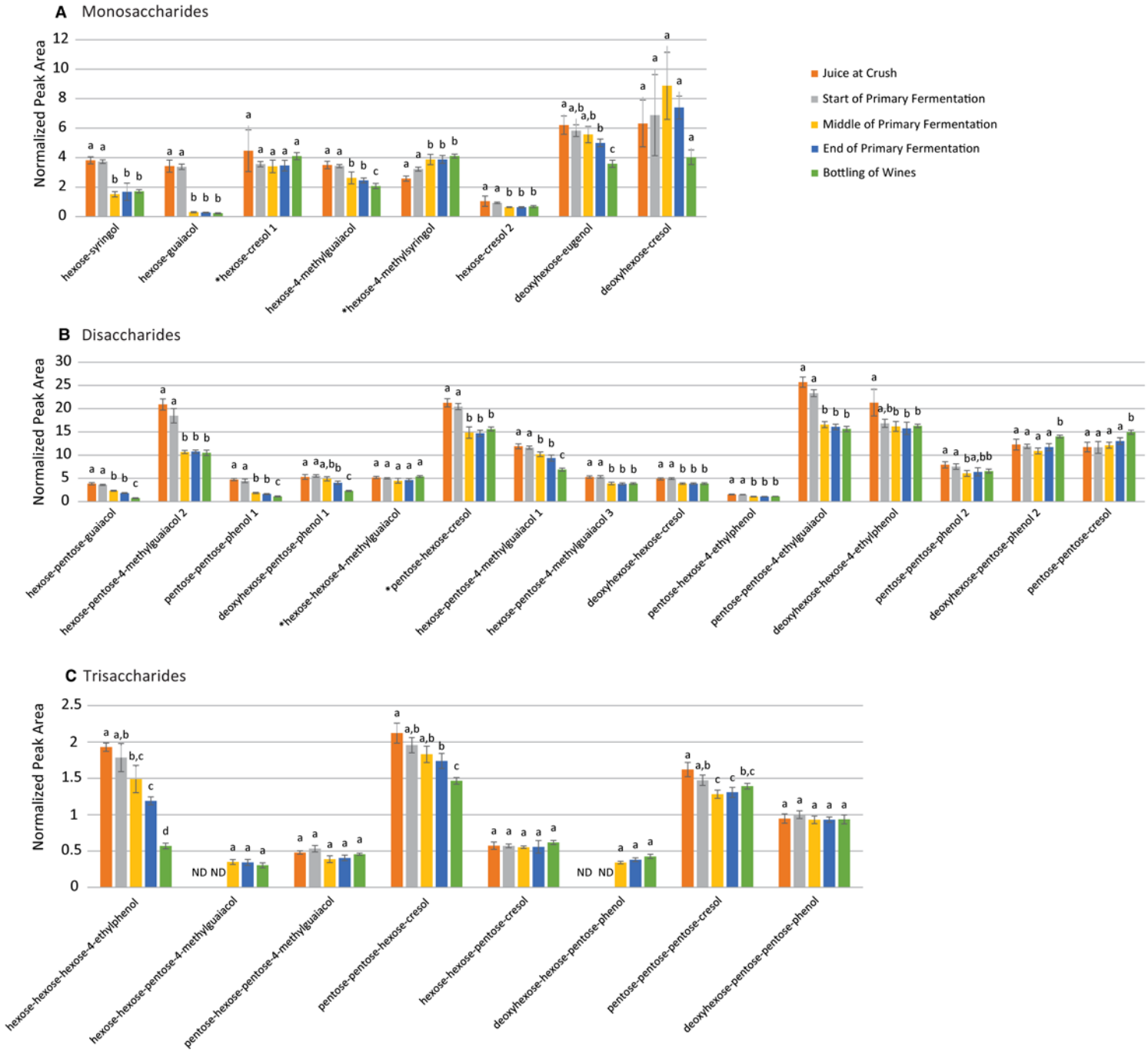

Figure 3 Relative abundance of volatile-phenol glycosides in smoke-exposed grapes and during fermentation. (**A**) monosaccharide glycosides, (**B**) disaccharide glycosides, and (**C**) trisaccharide glycosides. Abundances reported are based on normalization to the internal standard salicin. The following five fermentation time points are shown: the juice at crush, the start of primary fermentation (25.0 Brix), the middle of primary fermentation (12.5 ± 1.0 Brix), the end of primary fermentation (<0 Brix), and wine at the bottling stage post-malolactic fermentation and filtering. Error bars represent standard deviation for nine replicate analyses (3 fermentation replications × 3 analytical replications). Bars with the same superscript are not statistically different at $p < 0.05$. An (*) by the compound name denotes that the normalized peak area was divided by 10. A signal-to-noise (S/N) of 10 was used for the limit of quantitation. The hexose guaiacol peak (**A**) had an S/N ratio of 3 to 5 depending on the sample; we have included relative concentrations for this peak to provide insight on the overall extent of hydrolysis.

The largest changes in the composition of the volatile-phenol glycosides occurred during the first half of the primary fermentation, which is in accordance with the glycosidase activities of *Saccharomyces* yeast. *Saccharomyces* arabinosidases, rhamnosidases, and glucosidases are the most active at the start of the primary fermentation before they are deactivated by the ethanol content of the fermenting juice (Günata et al. 1986, Delacroix et al. 1994, Fia et al. 2005). After the enzymes were deactivated, no further changes in the abundance of volatile-phenol glycosides occurred during primary fermentation. Although the work was done through semi-quantitation, the results may still be compared to results reported by other authors. Kennison et al. (2008) reported the increase in abundance of free guaiacol, 4-methylguaiacol, 4-ethylguaiacol, and 4-ethylphenol throughout winemaking. By contrast, we showed a decrease in guaiacol, 4-methylguaiacol, 4-ethylguaiacol, and 4-ethylphenol glycoconjugates (Figure 3A and 3B). Although the study is limited by the absence of volatiles analysis and the lack of deuterated glycoside compounds, the changes in abundances are in similar levels to those reported by Kennison et al. (2008) when considering salicin had a concentration of 50 µg/L in each sample.

After the primary fermentation, the wines underwent malolactic fermentation, racking, and filtration before they were bottled. Although some compounds did decrease by 30% to 50% during this 6-mo time period, the overall changes (~5%) were very small compared to the average decrease of 23% observed due to the action of the yeast. Compounds such as hexose-hexose-hexose-4-ethylphenol (Figure 3C) may have had structures that were more susceptible to hydrolysis in the presence of the malolactic bacteria. The extent of hydrolysis was much less than expected based on previous reports (Kennison et al. 2008), which showed that malolactic fermentation increased the amount of free guaiacol and 4-methylguaiacol. This difference may be explained by the variable nature of malolactic bacteria. Previous studies that focus on the hydrolytic activity of *Oenococcus* bacteria show a large variation in hydrolytic activity between strains of bacteria, and this activity is dependent on factors such as juice/wine pH, ethanol content, and residual sugar content (Grimaldi et al. 2000, Barbagallo et al. 2004, Perez-Martin et al. 2012).

Approximately 72% of the volatile-phenol glycosides remained at the end of primary fermentation and prior to bottling (Figure 3). Although the scope of this study was limited and the results only infer the effect of changes in glycoside abundances on the respective free volatile compounds, they indicate a large remaining reservoir of glycosidic compounds that can affect the flavor of the wine as it ages and when it is consumed because acid hydrolysis may continue after bottling (Fudge et al. 2011, Ristic et al. 2017). Wine treatments such as reverse osmosis have been shown to attenuate the amounts of free volatile phenols in wine; however, reverse osmosis was unable to influence the abundances of volatile-phenol glycosides (Fudge et al. 2011). The presence of volatile-phenol glycosides in wine can also have an effect on the retronasal aroma of tainted wine. In-mouth hydrolysis of volatile-phenol glycosides has been shown to contribute to a notable aftertaste flavor within ~2 min of placing the samples in the mouth (Mayr et al. 2014). The flavor can also increase over time as in-mouth hydrolysis continues, thereby imparting undesirable flavors to wines that seemed otherwise normal through orthonasal aroma (Parker et al. 2012).

Conclusions

UHPLC coupled with MS/MS was used to identify and semi-quantitate volatile-phenol glycosides during the winemaking process. Thirty-one volatile-phenol glycosides were identified in grapes and fermenting wines along with the first instance where trisaccharide volatile-phenol glycosides have been tentatively characterized. The first half of the primary fermentation had the largest effect on the glycosidic profile of the fermenting wines. The abundances of some glycosides did decrease after pressing the wines and before bottling, but the exact mechanism for the decrease cannot be determined, as both microbial enzymes and acid hydrolysis may contribute. Approximately three-quarters of the smoke taint-related glycosides remained 5 mo after the end of primary fermentation. Further studies are needed to better understand how the changes in glycoside abundances correlate to changes in the abundances of related free volatiles. In addition, more information is needed about the effects of wine aging and different wine treatments on the abundances of volatile-phenol glycosides, particularly the trisaccharides. Finally, further sensory studies are needed to determine if the changes in composition at the different fermentation stages have significant effects on sensory properties of the wines.

Literature Cited

Barbagallo RN, Spagna G, Palmeri R and Torriani S. 2004. Assessment of β-glucosidase activity in selected wild strains of *Oenococcus oeni* for malolactic fermentation. Enzyme Microb Technol 34:292-296.

Bönisch F, Frotscher J, Stanitzek S, Rühl E, Wüst M, Bitz O and Schwab W. 2014. UDP-glucose:monoterpenol glucosyltransferase adds to the chemical diversity of the grapevine metabolome. Plant Physiol 165:561-581.

Delacroix A, Günata Z, Sapis JC, Salmon JM and Bayonove C. 1994. Glycosidase activities of three enological yeast strains during winemaking: Effect on the terpenol content of Muscat wine. Am J Enol Vitic 45:291-296.

Dungey KA, Hayasaka Y and Wilkinson KL. 2011. Quantitative analysis of glycoconjugate precursors of guaiacol in smoke-affected grapes using liquid chromatography–tandem mass spectrometry based stable isotope dilution analysis. Food Chem 126:801-806.

Dziadas M and Jeleń H. 2011. Influence of glycosides addition on selected monoterpenes contents in musts and white wines from two grape varieties grown in Poland. Acta Sci Pol Technol Aliment 10:7-17.

Fia G, Giovani G and Rosi I. 2005. Study of β-glucosidase production by wine-related yeasts during alcoholic fermentation. A new rapid fluorimetric method to determine enzymatic activity. J Appl Microbiol 99:509-517

Flamini R, De Rosso M, Panighel A, Dalla Vedova A, De Marchi F and Bavaresco L. 2014. Profiling of grape monoterpene glycosides (aroma precursors) by ultra-high performance-liquid chromatography-high resolution mass spectrometry (UHPLC/QTOF). J Mass Spectrom 49:1214-1222.

Fudge AL, Ristic R, Wollan D and Wilkinson, KL. 2011. Amelioration of smoke taint in wine by reverse osmosis and solid phase adsorption. Aust J Grape Wine Res 17:S41-S48.

Grimaldi A, McLean H and Jiranek V. 2000. Identification and partial characterization of glycosidic activities of commercial strains of the lactic acid bacterium, *Oenococcus oeni*. Am J Enol Vitic 51:362-369.

Günata YZ, Bayonove CL, Baumes RL and Cordonnier RE. 1986. Stability of free and bound fractions of some aroma components of grapes cv. Muscat during the wine processing: Preliminary results. Am J Enol Vitic 37:112-114.

Hayasaka Y, Baldock GA, Pardon KH, Jeffery DW and Herderich MJ. 2010a. Investigation into the formation of guaiacol conjugates in berries and leaves of grapevine *Vitis vinifera* L. cv. Cabernet Sauvignon using stable isotope tracers combined with HPLC-MS and MS/MS analysis. J Agric Food Chem 58:2076-2081.

Hayasaka Y, Dungey KA, Baldock GA, Kennison KR and Wilkinson KL. 2010b. Identification of a β-D-glucopyranoside precursor to guaiacol in grape juice following grapevine exposure to smoke. Anal Chim Acta 660:143-148.

Hayasaka Y, Parker M, Baldock GA, Pardon KH, Black CA, Jeffery DW and Herderich MJ. 2013. Assessing the impact of smoke exposure in grapes: Development and validation of a HPLC-MS/MS method for the quantitative analysis of smoke-derived phenolic glycosides in grapes and wine. J Agric Food Chem 61:25-33.

Hjelmeland AK, Zweigenbaum J and Ebeler SE. 2015. Profiling monoterpenol glycoconjugation in *Vitis vinifera* L. cv. Muscat of Alexandria using a novel compound database approach, high resolution mass spectrometry and collision induced dissociation fragmentation analysis. Anal Chim Acta 887:138-147.

Kennison KR, Wilkinson, KL, Williams HG, Smith JH and Gibberd MR. 2007. Smoke-derived taint in wine: Effect of postharvest smoke exposure of grapes on the chemical composition and sensory characteristics of wine. J Agric Food Chem 55:10897-10901.

Kennison KR, Gibberd MR, Pollnitz AP and Wilkinson KL. 2008. Smoke-derived taint in wine: The release of smoke-derived volatile phenols during fermentation of Merlot juice following grapevine exposure to smoke. J Agric Food Chem 56:7379-7383.

Kennison KR, Wilkinson KL, Pollnitz AP and Williams HG, Gibberd MR. 2009. Effect of timing and duration of grapevine exposure to smoke on the composition and sensory properties of wine. Aust J Grape Wine Res 15:228-237.

Mayr CM, Parker M, Baldock GA, Black CA, Pardon KH, Williamson PO, Herderich MJ and Francis IL. 2014. Determination of the importance of in-mouth release of volatile phenol glycoconjugates to the flavor of smoke-tainted wines. J Agric Food Chem 62:2327-2336.

Noestheden M, Dennis EG, Romero-Montalvo E, DiLabio GA and Zandberg WF. 2018. Detailed characterization of glycosylated sensory-active volatile phenols in smoke-exposed grapes and wine. Food Chem 259:147-156.

Parker M et al. 2012. Contribution of several volatile phenols and their glycoconjugates to smoke-related sensory properties of red wine. J Agric Food Chem 60:2629-2637.

Pérez-Martin F, Seseña S, Izquierdo PM, Martin R and Palop ML. 2012. Screening for glycosidase activities of lactic acid bacteria as a biotechnological tool in oenology. World J Microbiol Biotechnol 28:1423-1432.

Ponzini E, Borgonovo G, Merlini L, Galante YM, Santambrogio C and Grandori R. 2015. Quantification of sugar epimers in polygalactomannans by ESI-MS/MS. J Anal Bioanal Tech 6:281.

Ristic R, Osidacz P, Pinchbeck KA, Hayasaka Y, Fudge AL and Wilkinson KL. 2011. The effect of winemaking techniques on the intensity of smoke taint in wine. Aust J Grape Wine Res 17:S29-S40.

Ristic R, van der Hulst L, Capone DL and Wilkinson KL. 2017. Impact of bottle aging on smoke-tainted wines from different grape cultivars. J Agric Food Chem 56:4146-4152.

Sarry JE and Günata Z. 2004. Plant and microbial glycoside hydrolases: Volatile release from glycosidic aroma precursors. Food Chem 87:509-521.

Tikunov YM, de Vos RCH, González Paramás AM, Hall RD and Bovy AG. 2010. A role for differential glycoconjugation in the emission of phenylpropanoid volatiles from tomato fruit discovered using a metabolic data fusion approach. Plant Physiol 152:55-70.

Wilkinson KL et al. 2011. Comparison of methods for the analysis of smoke related phenols and their conjugates in grapes and wine. Aust J Grape Wine Res 17:S22-S28.